Tests of SARG, the High Resolution Spectrograph for TNG

Raffaele Gratton[1], Giovanni Bonanno[2], Pietro Bruno[2], Antonio Calì[2], Riccardo Claudi[1], Rosario Cosentino[2], Silvano Desidera[3], Giancarlo Farisato[1], Giorgio Martorana[1], Mauro Rebeschini[1], Salvatore Scuderi[2], Maria Cristina Timpanaro[2]

[1]Osservatorio Astronomico di Padova, Vicolo dell'Osservatorio 5, 35122 Padova, ITALY
[2]Osservatorio Astrofisico di Catania, Viale Andrea Doria, 95100 Catania, ITALY
[3]Dipartimento di Astronomia, Universita' di Padova, Vicolo dell'Osservatorio 5, 35122, ITALY

ABSTRACT

We present results of laboratory tests of the high resolution spectrograph (SARG), that will be soon in operation at TNG telescope, La Palma. These first results shows that the instruments performs according to specifications, providing the expected very high resolution; and that can be operated remotely according to the TNG standards

Key words: Instrumentation: spectrograph - Instrumentation: optical

1. INTRODUCTION

SARG is the high resolution spectrograph for the Galileo National Telescope. Istrument specifications included a high spectral resolution (maximum about $R \sim 150,000$), high efficiency (peak at more than 15%), rather large spectral coverage in a single shot (two shots allowing to cover the entire accessible range from 370 to 900 nm; UV was sacrified due to to budget limitations), high stability (long term stability of 5 m/s, and possibly 1 m/s over a single night). While meeting all these requirements required a complex and sophisticated instrument, design criteria also included simplicity of use and maintenance, and respect for the TNG standards and environment.

Three years after its approval, SARG was tested in its own specially devoted optical laboratory in Padova. Now it has been moved to La Palma, where it will be mounted at the telescope during summer 2000.

SARG is a collaboration of the astronomical observatories of Padova (optics, mechanics, thermal control, integration, science verification, project management), Catania (controls, software, detectors), Trieste and Palermo (management and science verification).

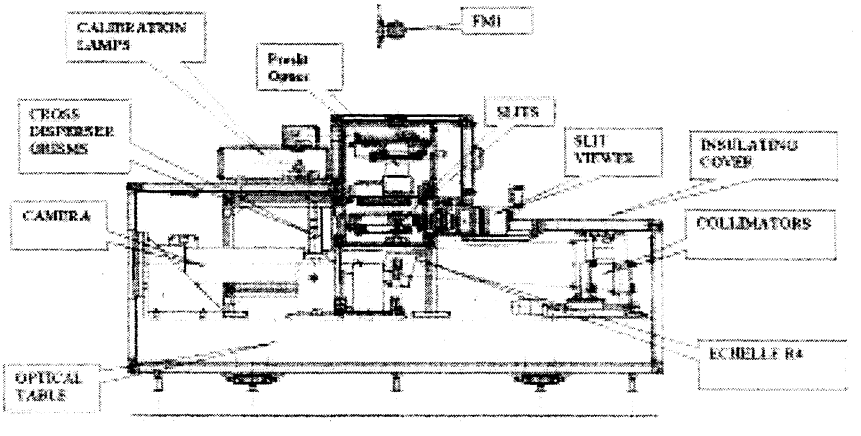

Figure 1. Mechanical layout of SARG. The main subsystem are labeled

In *Optical and IR Telescope Instrumentation and Detectors*, Masanori Iye, Alan F. M. Moorwood, Editors, Proceedings of SPIE Vol. 4008 (2000) • 0277-786X/00/$15.00

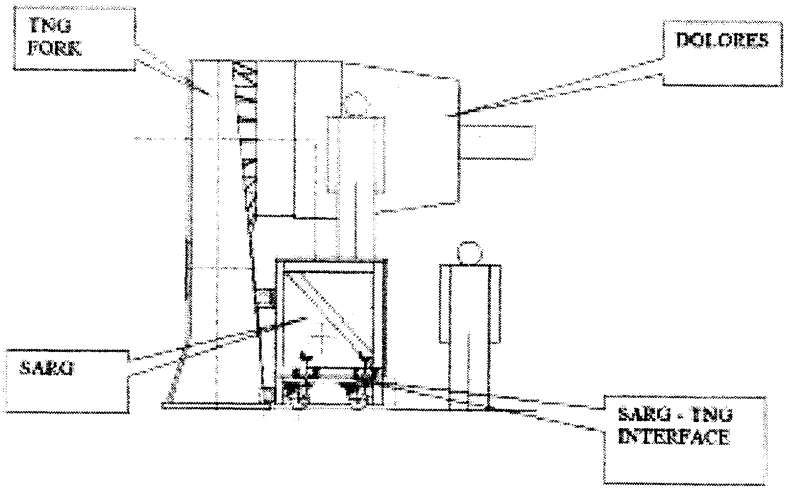

Figure 2. SARG location on the TNG arm B

2. TECHNICAL CHARACTERISTICS

The general layout of SARG is shown in Figure 1. SARG is mounted on an optical table rigidly attached at the fork of TNG, about 1.4 m below the Nasmyth B focus (see Figure 2). Light reaches the spectrograph through an optical train which includes three lenses (L1, L2, and L3), and a folding mirror (FM1) which redirects light exiting horizontally along the elevation axis downward to the spectrograph location. L1 and FM1 are mechanically located within DoLoRes (the TNG low dispersion spectrograph) which permanently occupies the Nasmyth B location.

In analogy with several modern high resolution spectrographs, SARG has a white pupil collimator. This design, coupled with the use of an R4 echelle, of grism cross dispersing elements, and of a large field, quite long focal length dioptric camera exploiting a large size detector, composed of a mosaic of 2 $2k \times 4k$ CCDs, pixel 13.5 μm, allowed a very compact and simple mechanical design. Instrument size is about $2 \times 1 \times 1$ m, very small in view of the high spectral resolution achieved by the instrument when mounted on a 3.5 m telescope. This compact design also simplifies its thermal design: a special feature of SARG is its distributed active thermal control system (DATCS), which should allow the spectrograph to have a nearly constant temperature of 20 ± 0.5 C.

The preslit optics (which includes a collimated part of the optical path) and the grism cross disperser also add flexibility to SARG, allowing a variety of optical modes: multiorder short slit observations with a large spectral coverage; 30 arcsec single order long slit observations (an optical derotator allows to have an arbitrary fixed orientation of the slit projected on the sky); multiorder image slicer observations at very high spectral resolution, using a Diego modified Bowen - Walraven image slicer; high precision radial velocity observations using an I_2 absorbing cell.

3. LABORATORY TESTS

SARG has been aligned in our optical laboratory during summer 1999, using a Taylor-Hobson MAT telescope coupled with a Electrim CCD, with a special software (ALISA) developed by Spot. During the same period, mechanics, controls and software were also completed, so that full tests of SARG functionalities were possible.

During last autumn we had two test runs (the first in September, the second one in December). During these runs, we tested optics, mechanics, controls, software, detectors, and the thermal behavior of SARG. Note that at epoch of these tests, only one of the two CCD's of the focal plane mosaic is available (the second is now being mounted on the mosaic). Additionally, the image slicer (realized by the University College of London) is still not available, so that the maximum resolution during these test was 112,600 (nominal at order center). Spectra of calibration lamps and of the Sun (through a fiber link) were acquired. We generally find that the instrument worked according specifications.

Examples of these spectra are shown:

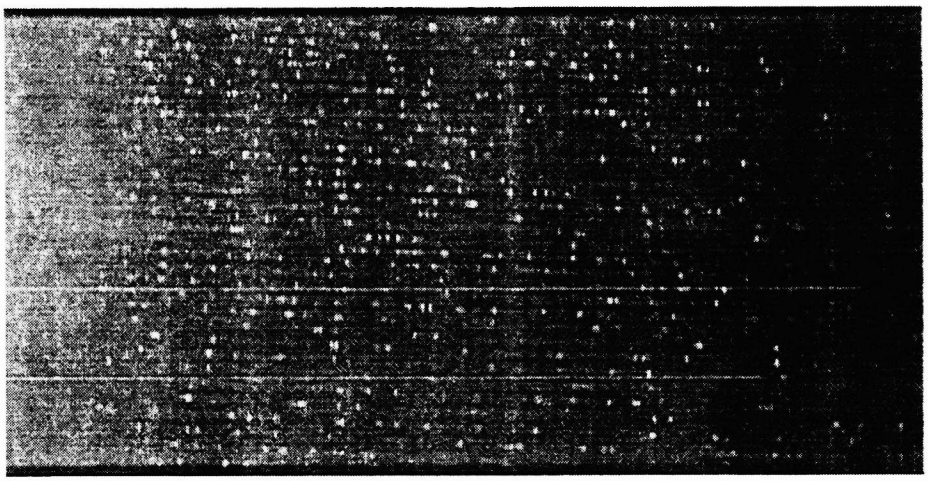

Figure 3. Spectrum of the Th lamp, acquired with the yellow grism; the slit aperture width was 75 μm, yielding a nominal spectral resolution of 112.600

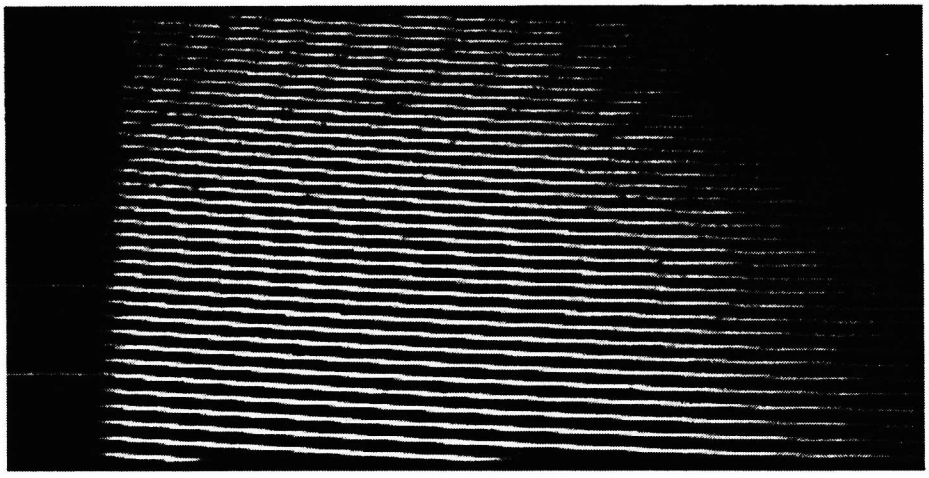

Figure 4. Solar spectrum acquired with the yellow grism; the slit aperture width was 75 μm, yielding a nominal spectral resolution of 112.600

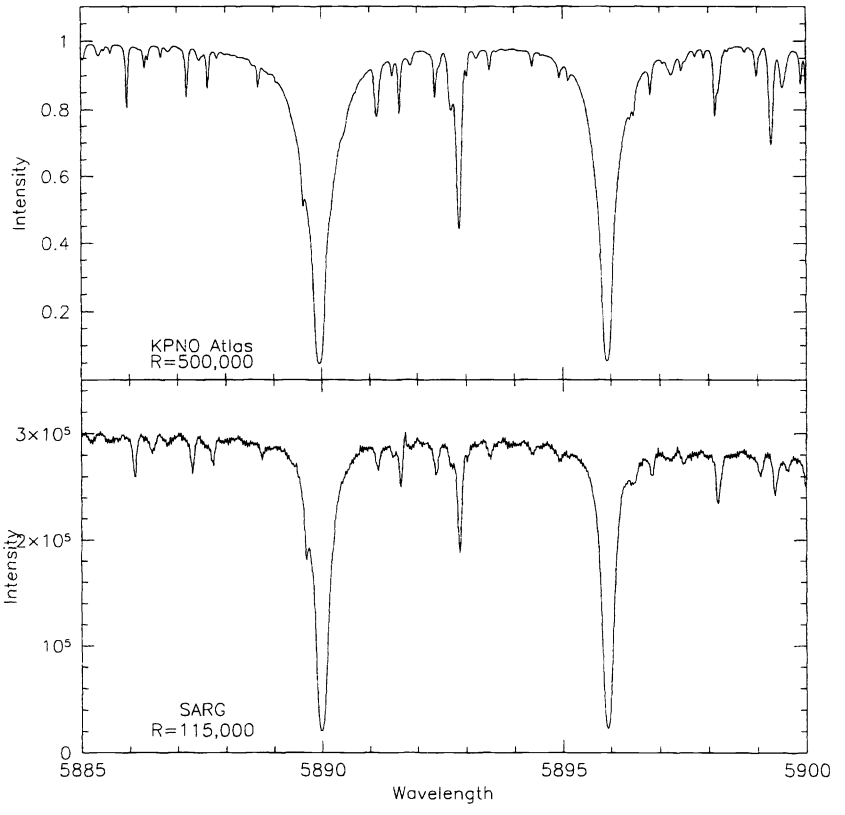

Figure 5. Plot of the solar spectrum around the Na D lines, as given by the Solar Atlas by Kurucz et al. (1984: upper panel), and as obtained using SARG (lower panel) at a nominal spectral resolution of 112,600

- Figure 3: portion of the spectrum of the Th lamp, acquired with the yellow grism; the slit aperture width was 75 μm, yielding a nominal spectral resolution of 112,600
- Figure 4: portion of the solar spectrum acquired with the yellow grism; the slit aperture width was 75 μm, yielding a nominal spectral resolution of 112,600
- Figure 5: plot of the solar spectrum around the Na D lines, as given by the Solar Atlas by Kurucz et al. (1984: upper panel), and as obtained using SARG (lower panel) at a nominal spectral resolution of 112,600

3.1. Optics

3.1.1. Resolution and spectral coverage

We used IRAF to wavelength calibrate the Th lamp and solar spectra obtained during the test run using the yellow grism (4570–6180 Å, orders 134–100 when using a single CCD). The final r.m.s. value of residuals (about 2,000 lines, using a Chebishev bidimensional polynome of orders 5 and 4) is 0.0015 Å(corresponding to an r.m.s. accuracy of about 84 m/s in radial velocities from individual lines). We also carefully measured the dispersion within order 118, centered at 5196.56 Å. At order center, the dispersion along CCD columns resulted to be 0.01888 Å/pixel, that is 1.3982 Å/mm. However, we find that dispersion forms an angle of about 0.7 degrees with the CCD columns (see below). Once this factor is taken into account, the measured linear dispersion at center of order 118 is 1.3981 Å/mm. If we then take into account the camera focal length, we found that the angle of illuminance of the echelle in the configuration used in the laboratory is 75.38 degree. This is about 0.3 degrees larger than the blaze angle measured

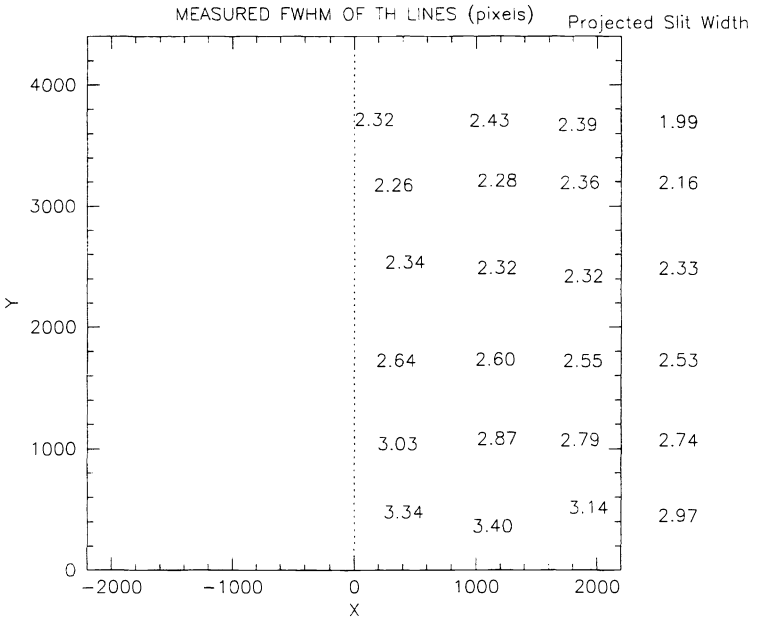

Figure 6. FWHM (in pixels) of the Th lines in different positions on the detector. At the nominal resolution, the projected slit width was 2.445 pixels at order centers; due to the anamorphic magnification of the echelle, the projected slit width is expected to change by about ±20% at the extremes of the orders visualized on the detector

for the R4 master (=75.09 degree). We then expect the maximum of the blaze function to be at about 0.6 degree (i.e. about 400 pixels) blueward of order center, as we actually observed. From the measured central wavelength of order 118 we also determined the value for the echelle grating constant to be 31.55 gr/mm.

3.1.2. Projected slit width

Since SARG uses a quasi-Littrow configuration, projected slit width at order center is simply the real slit width times the ratio (=0.4409) between the camera and collimator focal lengths (485 and 1100 mm respectively). Out of order center, this width should be multiplied for the anamorphic factor $A = \cos\alpha/\cos\beta$, where α and β are the incidence and refracted angles respectively. While α should coincide with the the echelle blaze angle (75.09 degrees), we actually adopted $\alpha = 75.38$ degree in the configuration used in the laboratory; the large detector size (4096 pixel) allows a large coverage along each order ($72.12 < \beta < 78.64$). We then have $0.822 < A < 1.281$ for the anamorphic factor.

The narrower slit used during our laboratory tests has a width of 75 μm. Neglecting degradation due to optical quality, the projected slit width is expected to be 2.445 pixels at order centre (this corresponds to a resolution of $R = 112,600$), and to be 2.01 pixels at one order extreme and 3.13 pixels at the other extreme.

Figure 6 compares the actual FWHM (in pixels) measured on a Th lamp spectra, obtained with this narrow slit, with values expected for SARG. The comparison is excellent and shows that SARG optics do not cause a serious degradation of the optical quality even at high resolution (actually, near order center the projected slit width coincides with the measured FWHM).

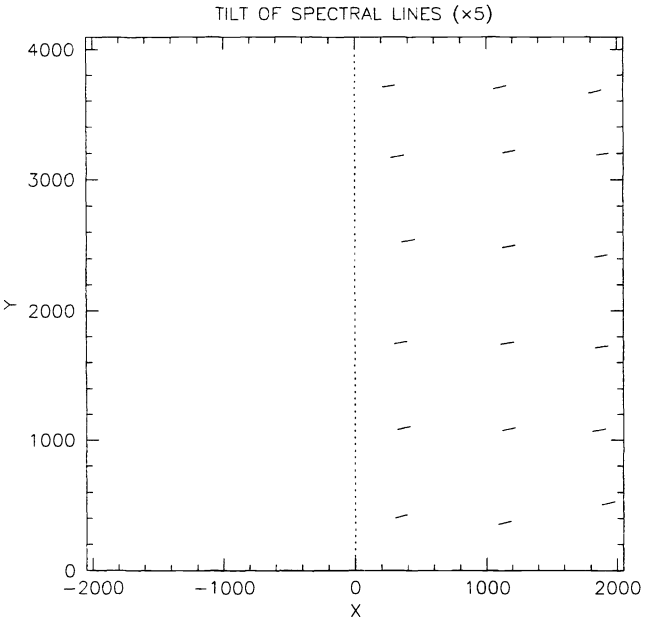

Figure 7. Tilt of Th lines in different positions on the detector. To show tilting more clearly, vertical scale has been exaggerated by a factor of 5

3.1.3. Order tilting

In cross dispersed echelle spectrographs, orders are tilted by the ratio between the (angular) dispersion of the cross disperser and of the echelle. Since for both grisms and echelle dispersion depends on wavelength, tilting is different for each order. Additionally, due to large anomorphosis of the echelle spectra, orders are also curved, a quite strong effect for SARG.

We measured order tilting with respect to the CCD columns at the center of orders on a spectrum taken with the *yellow* grism; we expected it to be 1.51 degrees. The observed value is 2.20 degree: the difference of 0.69 degree is due to a rotation of the detector coordinate system.

3.1.4. Line tilting

In post-dispersed echelle spectrographs like SARG, lines are tilted with respect to the normal to dispersion by a constant value given by:

$$\frac{d\beta}{d\gamma} = \tan\gamma\,\lambda\,\frac{d\beta}{d\lambda}, \tag{1}$$

where β is the refracted angle and γ is the off-plane angle. In SARG design, the echelle is used in quasi-Littrow configuration, with an off plane angle $\gamma = 0.65$ degree. Lines are then expected to be tilted by a constant value of 5.0 degree with respect to dispersion; this tilting can be removed by a proper alignment of the slits.

Figure 7 gives values of line tilts with respect to CCD rows on the spectra acquired in the laboratory measured at different location on the focal plane. As expected, there is no obvious change of tilting along the orders (while

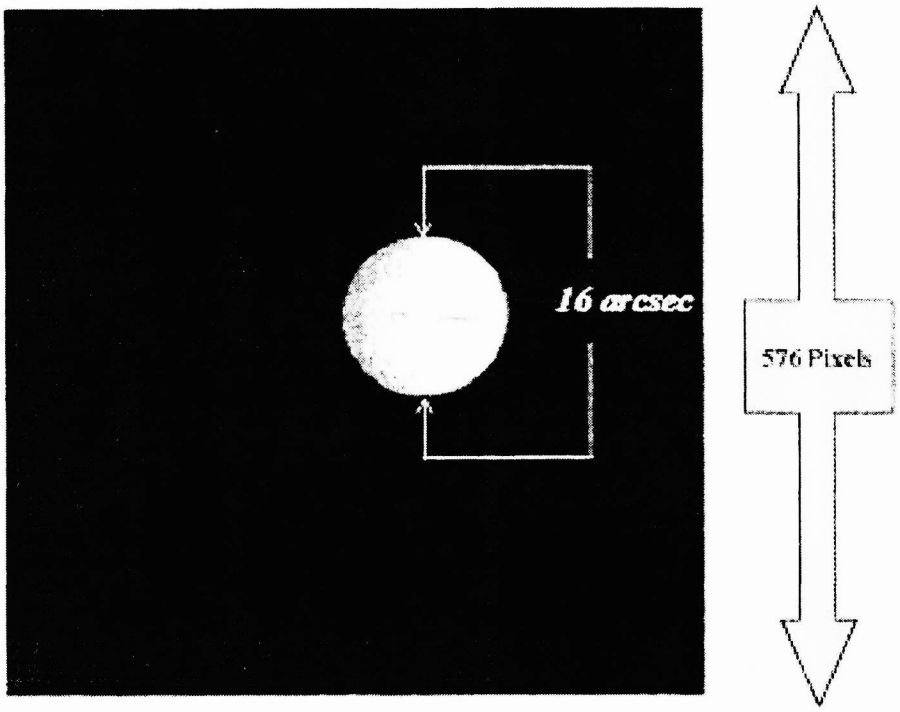

Figure 8. The R=112,600 slit illuminated by a flat field lamp, as acquired by the slit viewer CCD.

some distortion is present). The average measured tilting with respect to the CCD rows is 2.54 degree. While small (and thus not affecting spectral resolution), the residual tilting of lines with respect to the CCD rows may well be removed during final alignment of spectrograph at the telescope.

3.2. Slit viewer

The slit viewer is based on a scientific camera, equipped with one CCD EEV0520 (770 × 1152) frame transfer, a slit wheel with nine apertures, a pick up optics and a movable turret. The wheel contains six reflecting plates with the slits, an image slicer, one pinhole and one mirror. The movable turret contains an objective and an array of 22 × 22 lens for the Schack-Hartmann analysis, that can be alternatively put on the optical path in front of the CCD.

Functionality of the slit viewer was tested during the December test run. An example of an image acquired with the slit viewer is given in Figure 8. When at TNG, the slit viewer CCD will be directly interfaced with the motor VME.

3.3. Controls

SARG controlled functions include nine motorized movements, seven lamp functions and eight temperature monitors. Low level controllers driving these functions are commanded by the SARG VME under GATE environment, by means of RS-232 connections and a Baytech multiplexer. The VME, the controllers and the power supplies are located in the SARG electronics cabinet. Test and debugging of individual motorized functions may also be carried on using a stand alone PC-software. The scheme of the VME-based SARG controls is illustrated in Figure 9, while the scheme of the individual controlled functions, driven by the controllers operated through the Baytech multiport is shown in Figure 10

All these functions were extensively tested. In particular, movement accuracy and repeatibility shows to be well within specifications, and have been tested over a very large number of cycles.

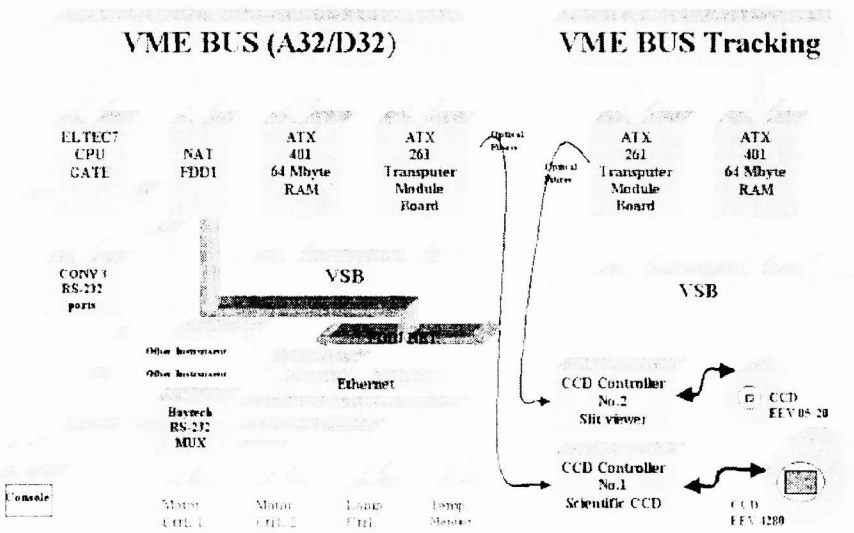

Figure 9. The scheme of VME-based SARG controls

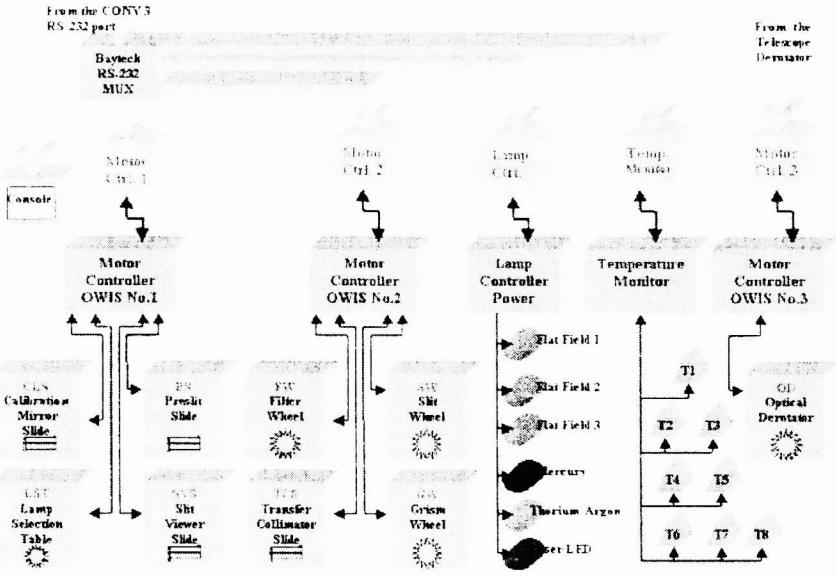

Figure 10. The scheme of the individual controlled functions, driven by the controllers operated through the Baytech multiport

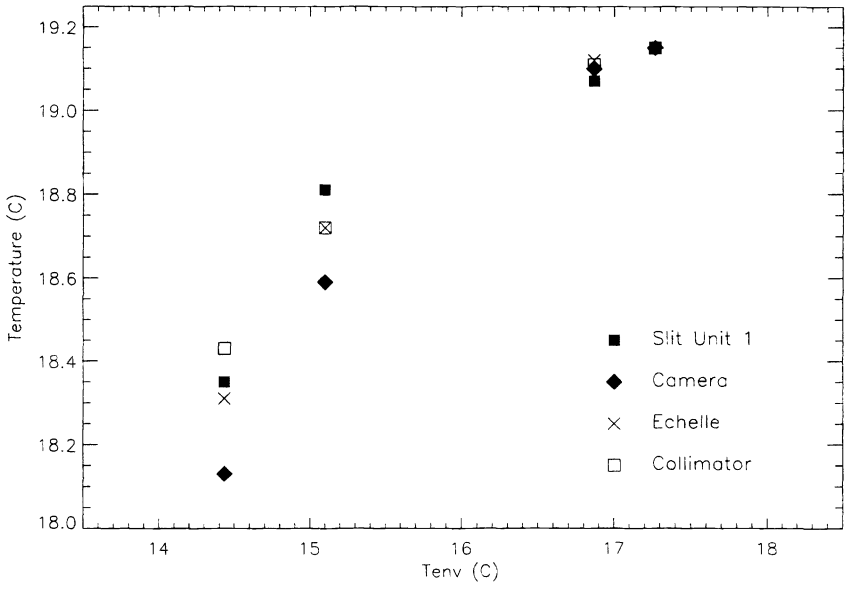

Figure 11. Temperature of Slit Unit1, Camera, Echelle and Collimator as a function of environment temperature. Note the different sensitivity of different parts of the instrument, likely due to camera+dewar thermal losses

3.4. Thermal Control

Temperature within the SARG enclosure is kept at 20 ± 0.5 C by means of a distributed active thermal control system (DATCS). The design of this system was done using a computer model. To achieve specifications, DATCS architecture consists of an array of 30 MINCO CT 198 HEATERSTAT sensorless temperature controllers coupled with thermofoil resistances, and of 8 DT-470 silicon diode sensors controlled by a Lakeshore 208 temperature. Within this design, particulare care was devoted to DATCS calibration. To this purposes, a special Heaterstat Calibration Box was constructed, a calibration procedure was defined and strictly enforced, and a maintenance plan was defined in order to mantain conditions stable over a long period of time.

SARG thermal control was tested in Padua Laboratory. Thermal equilibrium was reached after 30 hours, due to the very high thermal capacity of the spectrograph. This fact should also guarantee a short term (i.e. during a night) thermal stability at a very high level (variations less than 0.1 C) in working conditions.

The dependence of SARG temperature on external one was tested decreasing laboratory temperature from 17.3 to 14.4 C The resulting variations of temperature at different locations within SARG are shown in Fig 11. A temperature gradient along the optical axis is present, suggesting that thermal losses due to camera+dewar are dominating and not properly taken into account in our thermal model. More precisely, the dependence on T_{env} results 0.34 C/C, 0.28 C/C and 0.24 C/C for camera, echelle and collimator respectively. This does not match specifications; thus we are currently improving thermal insulation including a insulating enclosure all around the dewar.

3.5. Detectors

SARG detector is a mosaic of 2 thinned back-illuminated EEV 4280 CCD's, 2048×4096 pixel, pixel size 13.5 μm. The dark area between the two CCD's is about 400 μm. Note that echelle dispersion is roughly aligned along CCD columns; the missed spectral range can be observed using a different cross dispersing grism. Both CCD's are now available (the second one was delivered after the december test run). The CCD's are operated by a standard CTR-01 TNG controller, built by Elettromare. Biases V_{dd} and V_{rd} may be set independently for the two chips to optimise the operating conditions of each detector. Simultaneous readout by four outputs is possible. Time required for pixel processing and acquisition is 22 μs; total time for acquisition of a complete $4,096 \times 4,096$ image using four

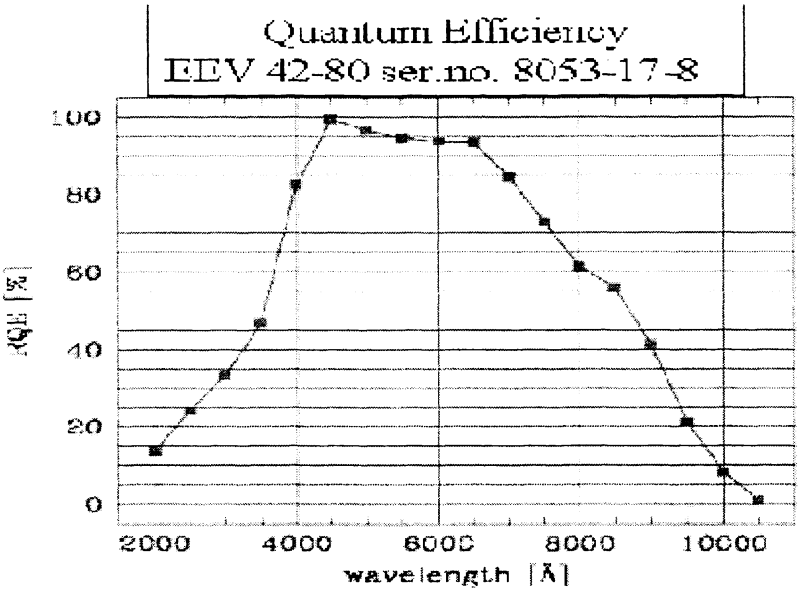

Figure 12. Measured quantum efficiency of the SARG CCD's as a function of wavelength

outputs is 93 seconds. Implemented software selectable binning modes are 1 × 1, 1 × 2, 1 × 4, 2 × 1, 2 × 2, 2 × 4, 4 × 1, 4 × 2, and 4 × 4; windowing of CCD's is also possible. Full characterization of the chips was made at the Catania Observatory COLD laboratory. The total system gain has been settled to have a conversion factor for each CCD of 1.294 e^-/ADU (measured with a ^{55}Fe X-ray source). The measured charge transfer efficiency is 0.9999998. Measured quantum efficiency is given in Figure 12. The readout noise of both devices is about 6 e^- r.m.s.. The ADC saturation is about 82,000 e^-, corresponding to 57% of the pixel full well capacity: no deviation from linearity is apparent within this range. Cosmetics of the chips is quite good, with only a few hot columns (<5 for each chip).

3.6. Software

Both low level software, residing on the VME and written within the TNG standard GATE environment, and the user interface (UIF), residing on a HP WS, and written in IDL language, are ready and tested. They were used to command the spectrograph during the December test run. As an example of the functionalities of this software (which allows complete remote control of the instrument), Figure 13 shows the main widget of the SARG UIF.

3.7. The Iodine Absorbing Cell

SARG is equipped with a iodine absorbing cell, the device that allows to obtain the highest radial velocity precision to date (Butler et al. 1996). Its high resolution (143000 using the image slicer), the complete spectral coverage of the range that contains the iodine lines in a single exposure, the mechanical and thermal stability coupled with the use of iodine cell make SARG a very competitive instrument in this field.

SARG iodine cell is a commercial component manufacted by Hellma, with path length 50 mm. Iodine filling was performed by G. Favero at Chemistry Department of Padua University. Sublimation temperature of iodine vapours was fixed at 46 C to obtain the desired optical depth. To obtain a proper working, the cell must be heated to a value higher than the sublimation value to avoid condensation of iodine on cold surfaces of the cell. From analysis of line depth at different temperatures, the final working temperature was fixed at 58 C. An appropriate thermal design ensures that overall thermal losses from iodine cell to SARG are within 2 W.

SARG iodine cell was tested during the laboratory runs performed at Padua Observatory in September and December 1999. The line depth at R=112600 results intermediate between UVES and HIRES cells. Fig 14 shows a small section of the spectra of pure iodine (with a FF lamp), pure star (the sun) and sun+iodine of the same spectral

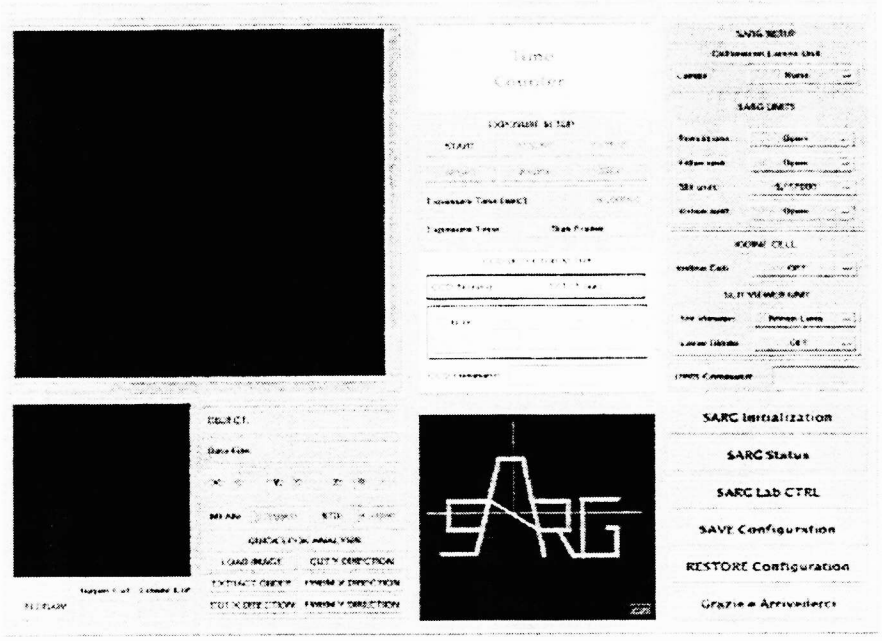

Figure 13. The main widget of the SARG UIF

region taken during SARG laboratory tests. Note the very dense forest of narrow iodine lines, that represent the wavelength reference superimposed onto stellar spectrum allowing to remove instrumental shifts.

Very high resolution iodine spectra required to model the spectrograph instrument profile were obtained at Kitt Peak FTS on 17-19 Nov 1999. The resolution is 0.02 cm^{-1}, corresponding to R=1000000 at 5000 Å and 750000 at 6500 Å.

The software we plan to use for SARG data is being developed at ESO by M. Kurster group (see Endl et al. 1999 for a preliminary report). It is not designed for a specific instrument but rather it is intended to be a very flexible tool, suitable for any spectrograph calibrated with an absorbing cell. The software includes instrument profile reconstruction, using a Maximum Entropy algorithm to properly model its asymmetries.

Acknowledgements

A number of discussions and data exchanges with M. Kurster was of invaluable utility in the analysis of SARG laboratory data. We thank H. Dekker and S. D'Odorico for permission of use of UVES iodine cell data. Thanks are due to M. Dulick for the very kind assistance during FTS run at Kitt Peak.

REFERENCES

1. Butler R.P., Marcy G.W., Williams E., McCarthy C., Dosahjh P & Vogt S.S., 1996, *PASP*, 108, 500
2. Endl M., Kurster M. & Els S., 1999, Poster Paper presented at *VLT Opening Symposium*
3. Kurucz, R.L., Furenlid, I., Brault, J. & Testerman, L., 1984, *Solar Flux Atlas from 296 to 1300 nm*, Cambridge, Harvard

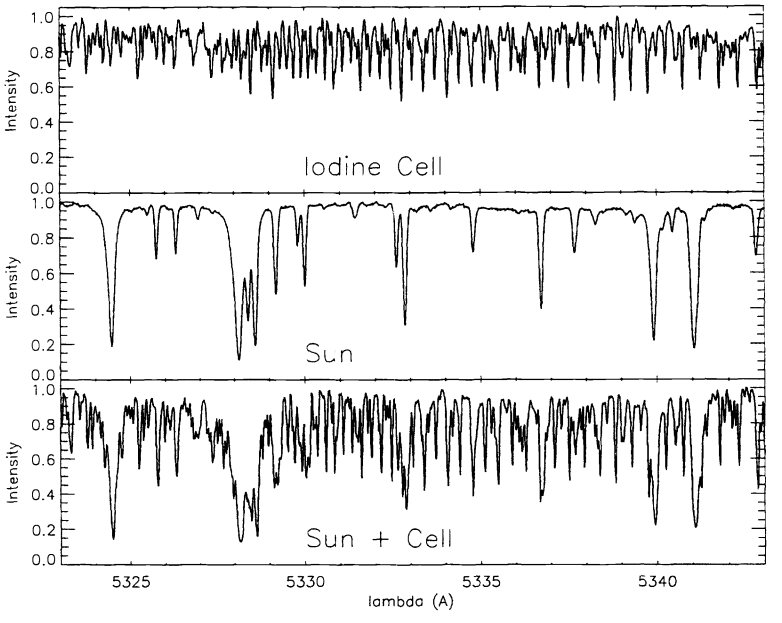

Figure 14. Spectra obtained with SARG during December 1999 run. Top panel: Iodine cell spectrum (with FF lamp), Median panel: Sun spectrum, Lower panel: Spectrum of the Sun + Iodine cell. Instrument configuration: R=112,600, Yellow Grism, T_{cell} = 56 C. The pure iodine spectrum has a bit less deeper lines than Sun+Cell one due the lack of background subtraction caused by order superposition with the used slit (note that there should not be order superposition at this wavelength when using the SARG image slicer)